

See discussions, stats, and author profiles for this publication at: <https://www.researchgate.net/publication/51780664>

Volatile Organic Compound Adsorption on a Nonporous Silica Surface: How Do Different Probe Molecules Sense the Same Surface?

ARTICLE in LANGMUIR · NOVEMBER 2011

Impact Factor: 4.46 · DOI: 10.1021/la203370c · Source: PubMed

CITATIONS

3

READS

14

4 AUTHORS, INCLUDING:



M. M. L Ribeiro Carrott

Universidade de Évora

113 PUBLICATIONS 2,561 CITATIONS

[SEE PROFILE](#)



Peter Carrott

Universidade de Évora

153 PUBLICATIONS 3,131 CITATIONS

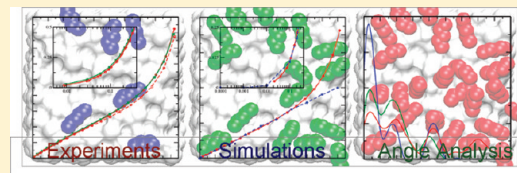
[SEE PROFILE](#)

Volatile Organic Compound Adsorption on a Nonporous Silica Surface: How Do Different Probe Molecules Sense the Same Surface?

Carmelo Herdes,^{*,†} M. Manuela L. Ribeiro Carrott,^{†,‡} Patrícia A. Russo,[†] and Peter J. M. Carrott^{†,‡}

[†]Centro de Química de Évora, and [‡]Departamento de Química, Universidade de Évora, 7000-671 Évora, Portugal

ABSTRACT: In this work, we compare experimental results to molecular simulation results of volatile organic compound (VOC) adsorption on nonporous silica. We adopted an effective model for the rough solid surface, obtained by a temperature annealing scheme, plus an experimental/simulation nitrogen adsorption tuning process over the silica energetic oxygen parameter. The measurement/prediction of selected VOCs, specifically, *n*-pentane and methylcyclohexane, is presented in terms of adsorption isotherms, with an emphasis on the angle distribution analysis of the three studied probe molecules with respect to the same modeled surface.



1. INTRODUCTION

The understanding of volatile organic compound (VOC) adsorption is crucial for the development of better strategies for controlling their industrial emissions,¹ because their undesired release into the atmosphere results in multiple health and environmental hazards. This subject is of particular interest in the scientific community, and worldwide environmental laws keep on enforcing the strict regulation of VOC venting. The challenge is also focused into achieving a clean technology that empowers an efficient handling of these compounds by means of both an appropriate adsorbent and the specific operational conditions, minimizing the risk of negligent vapor discharges and maximizing the economic profit. In that sense, any effort to enhance our knowledge in this area will have impact on global health by VOC emission control and, additionally, will empower the existent adsorbent market for recovery of the VOCs. An optimized recovery of reusable (or marketable) VOCs can significantly offset the cost of their emission control.² Appropriately designed adsorption systems can increase the concentration of VOCs to allow for either destruction by incineration or recovery by either membrane or condenser to be economically feasible.²

The working capacity of a given adsorbent is determined by operational factors, such as adsorbent bed size, preconditioning effects, desorption level, and regeneration time. At the same time, the retention capacity of the adsorption bed is determined by the given/desired concentration of VOC, the air flow rate, the mass of adsorbent in the bed, and the type of adsorbent. These operational and intrinsic characteristics of the adsorption bed are conditioned and interrelated by one major single variable, the available surface area (the area that a given adsorbate covers in a given adsorbent), with the former being the main subject of the present study: how do different probe molecules sense it?

Inorganic materials, such as silica, zeolites, carbonaceous materials, activated alumina, inorganic–organic materials, and molecularly imprinted polymers, have shown attractive characteristics for the adsorption of VOCs.^{3–13} The different adsorption properties between the materials are due to (i) their chemical composition

and (ii) their textural properties. With regard to the latter, most of the operative VOC adsorbents are essentially microporous. Nevertheless, at one point or another, the most common methods of isotherm analysis as well as molecular parameter fundamental definitions require reference data of the adsorbent under study on a nonporous solid. From the reference data, it is possible to calculate, for instance, α_s reduced data or statistical thickness of the adsorbed films or to obtain adsorbate–adsorbent interaction parameters. For nitrogen adsorption at 77 K, there is a relatively large amount of reference and standard data available in the literature. However, for some applications, nitrogen adsorption at 77 K is not sufficient or appropriate to achieve a complete characterization of porous solids. It is then necessary to exploit other adsorbents, such as organic vapors, and at higher temperatures. Reports on the adsorption of organic vapors on nonporous materials are scarce in the literature, particularly for silica materials. To help answer what governs VOC adsorption at the solid surface, in this work, we compare experimental results to molecular simulation results on a nonporous amorphous silica, determining a fingerprint analysis for a given single rough surface, on the basis of the different landing angles of various fluids.

2. METHODOLOGY

Aerosil 200 Pharma from Evonik Industries was selected as the fumed silica for the experimental studies. Prior to adsorption measurements, solid experimental samples were degassed for 8 h at 453 K, with the temperature achieved at a rate of 1 K/min, until a 9.0×10^{-6} mbar residual pressure was attained. The designations Aerosil200(823) and Aerosil200(1223) correspond to samples that were thermally treated for 8 h at 823 and 1223 K, respectively, temperatures achieved at a heating rate of 3 and 5 K/min, respectively.

Characterization by nitrogen adsorption at 77 K was performed as described elsewhere.¹⁴ Methylcyclohexane (>99%, Aldrich) and *n*-pentane

Received: August 27, 2011

Revised: October 13, 2011

Published: November 07, 2011

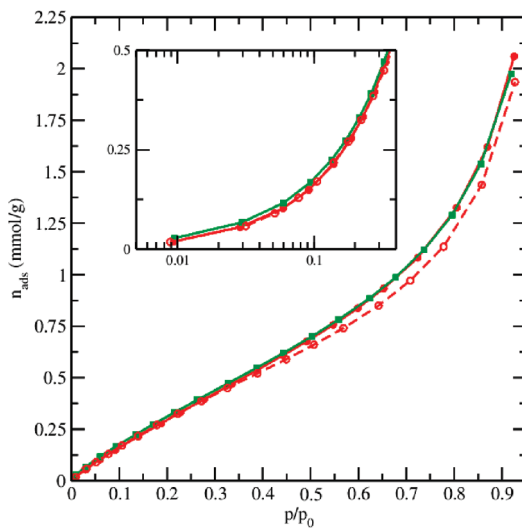


Figure 1. Experimental *n*-pentane adsorption isotherms at 298 K on nonporous silica: Aerosil200 (red solid circles and solid line), Aerosil200(823) (green solid squares and solid line), and Aerosil200(1223) (red open circles and dashed line). The inset presents the same data with pressures in logarithmic scale for a better inspection of the lower range.

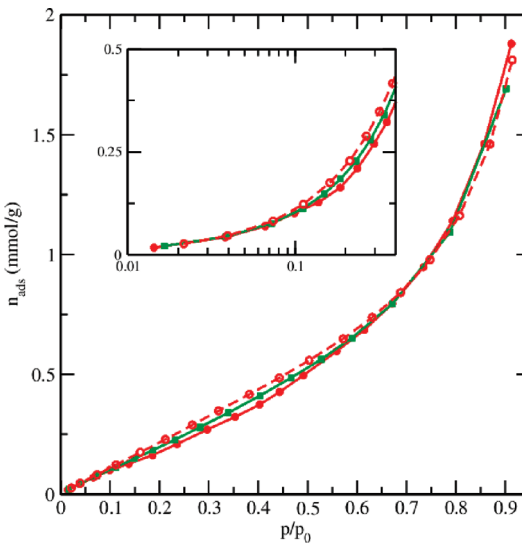


Figure 2. Experimental methylcyclohexane adsorption isotherms at 298 K on nonporous silica, following the description of Figure 1.

(99%, Lab-Scan) were the selected VOCs, outgassed in vacuum by repeated freeze–thaw cycles prior to the determination of the isotherms. The saturation pressure and density of the hydrocarbons at the working temperature were calculated from the Wagner and Rackett equations, respectively, and using data recommended in ref 15.

The VOC adsorption isotherms were determined gravimetrically in an apparatus equipped with a CI Electronics vacuum microbalance connected to a Disbal control unit and Edwards Barocel 622 (0–100 mbar) and 600 (0–1000 Torr) capacitance manometers. The temperature of the circulating liquid jacket around the balance tubes was controlled within ± 0.1 K using a Grant LTD thermostat and a Masterflex peristaltic pump. Blank measurements indicated that buoyancy corrections were negligible.

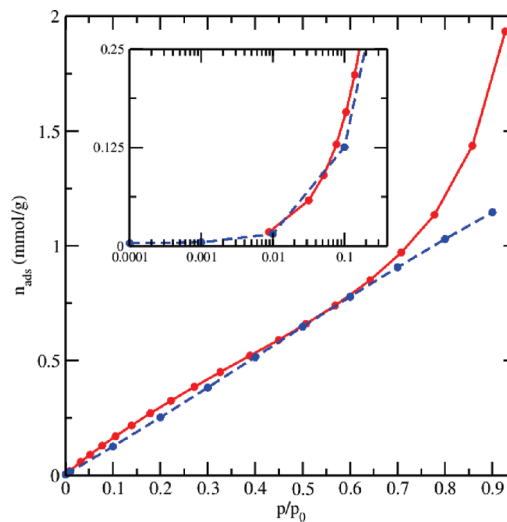


Figure 3. Experimental (red solid circles and solid line) and simulated (blue solid circles and dashed line) excess *n*-pentane adsorption isotherms at 298 K on nonporous silica.

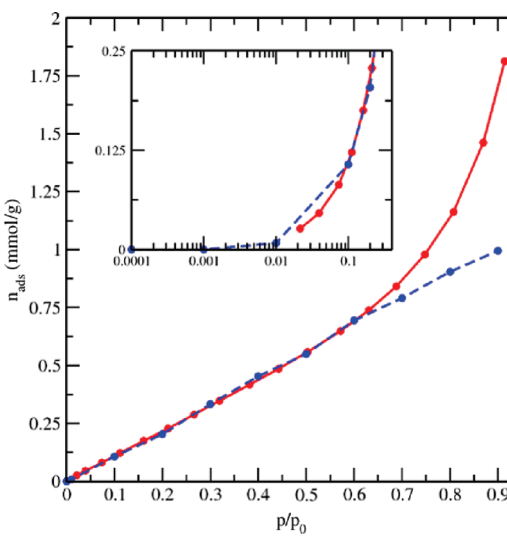


Figure 4. Experimental (red solid circles and solid line) and simulated (blue solid circles and dashed line) excess methylcyclohexane adsorption isotherms at 298 K on nonporous silica.

Recently, we compared experimental nitrogen adsorption isotherms to molecular simulation results on effective nonporous silica models.¹⁴ A molecular dynamic (MD) annealing temperature scheme was used for the formulation of different samples of the amorphous silica¹⁴ (a similar methodology based on Monte Carlo annealing can also be implemented).¹⁶ The comparison of the experimental and simulated nitrogen results was followed by a tuning process over the energetic parameter of the oxygen atoms of a selected structure.¹⁴ With the capitalization on that modeling strategy, the main characteristics of the proposed methodology are presented here; more details can be found in our previous work.¹⁴

The MD annealing scheme¹⁷ for the formulation of the solid surface model departs from a MD equilibrated bulk of SiO_2 (1600 oxygen + 800 silicon atoms) at 2000 K and 1 bar, in the NpT ensemble. The selected potential model was the modified Born–Mayer–Huggins interaction.¹⁸ The amorphous silica surface is obtained by quenching the liquid stepwise to the desired temperature. To induce the fracture, the bottom of

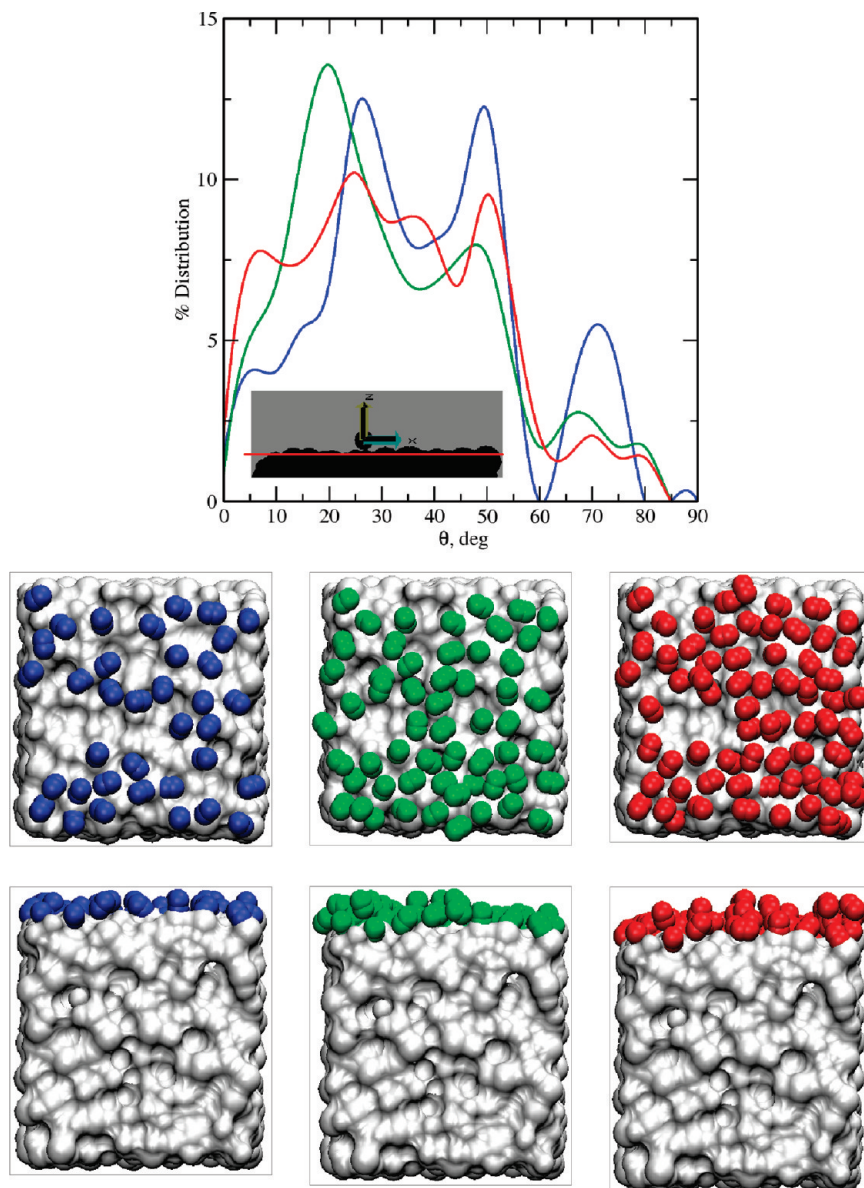


Figure 5. Percentage angle distribution for nitrogen at 77 K on nonporous silica for three levels of relative pressure 1×10^{-5} (blue), 4×10^{-3} (green), and 1×10^{-2} (red). Bottom snapshots, with high contrast colors, depict the molecules on the silica surface at each studied pressure (from left to right), with the first row a zenithal point of view and the second row a frontal point of view.

the simulation cell is frozen; meanwhile, an upper slab is allowed to reorganize facing vacuum.¹⁴ This methodology allows us to correlate the number of nonbridging oxygen (NBO) atoms and the accessible surface size with the imposed annealing temperature.¹⁴

All VOCs were mimicked as rigid structures with the TraPPE-(UA)^{19–25} forcefield, for the sake of a homogeneous model comparison. Although specific more advanced models do exist for each adsorptive but at different levels of development, the goal here, away from being the quantitative description of each specific system, is to ensure a common qualitative framework. Simulated adsorption isotherms were obtained by means of the well-established grand canonical Monte Carlo (GCMC) method.²⁶ This included four types of moves, specifically bias insertions and deletions,^{27,28} random rotations, and translations, with equal distribution of weights among the moves. The efficiency of sampling was achieved using the energy-biased GCMC protocol.²⁸ At least 5×10^7 GCMC steps were performed for each adsorption point, with each step being an attempt to insert, delete, rotate, or translate a

molecule. Half of the steps were taken to equilibrate the system, and the other half were taken to sample the data.

All cross-interactions were calculated using the simple Lorentz–Berthelot mixing rules. Nonbonded interactions were cut off at 1.5 nm. Adsorption data are presented as the excess fluid density adsorbed in the silica models (mmol/g) versus the relative pressure p/p_0 of the bulk phase, where p_0 is the bulk saturation pressure at the set temperature. Fugacities and gas-phase densities at the particular bulk conditions (temperature and pressure) were calculated using the well-known Peng–Robinson equation of state.

A landing angle analysis was performed to investigate how different probe molecules sense the same surface. In other words, to determine the orientation of a given molecular vector (**mv**) to the surface, in terms of the smallest angle between the **mv** and the *xy* plane of the simulation cell. The **mv** is defined between the center of mass of the two nitrogen beads, between the initial and final beads of the *n*-pentane chain, and between the methyl bead and the opposite methylene bead in the hexagonal

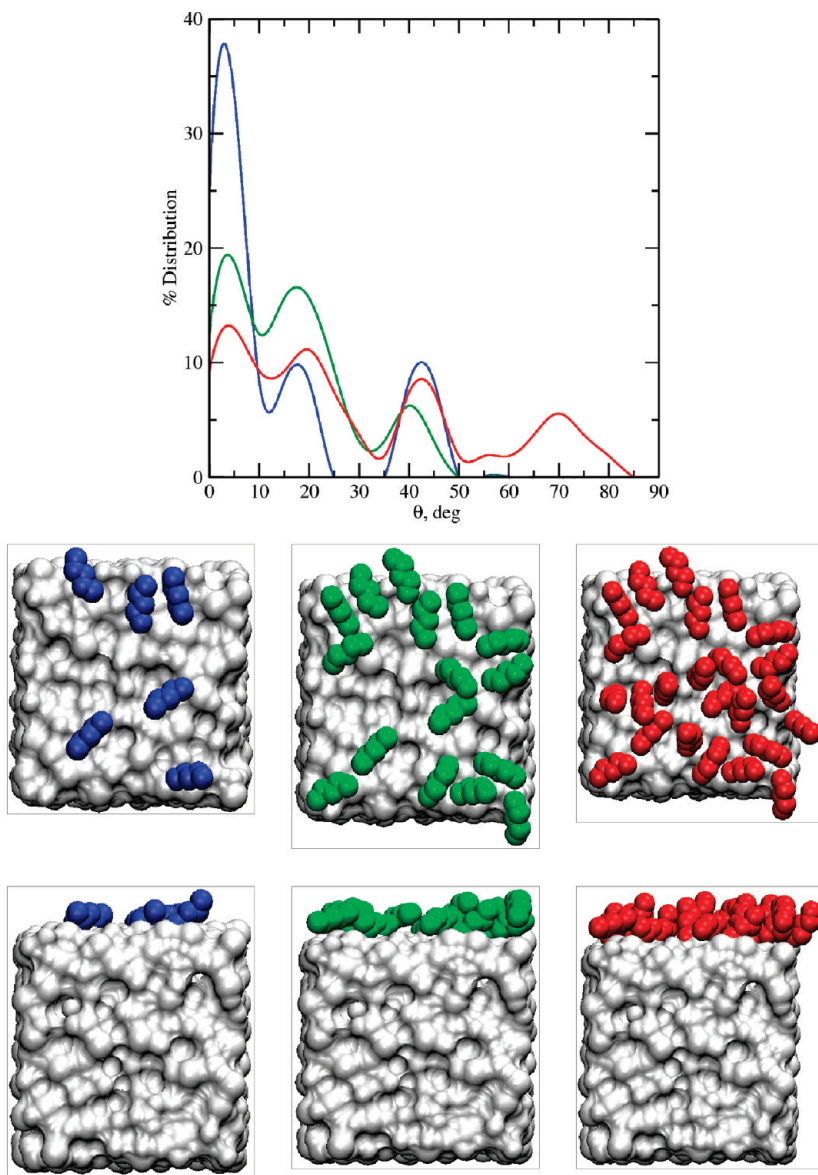


Figure 6. Percentage angle distribution for *n*-pentane at 298 K on nonporous silica for three levels of relative pressure: 0.1 (blue), 0.2 (green), and 0.3 (red), following the description of Figure 5.

ring of the methylcyclohexane molecule. In the analysis, 0° will correspond to a parallel molecule orientation; meanwhile, 90° will refer to a perpendicular molecule orientation with respect to the silica surface *xy* plane. MD NVT simulations, at the conditions of equilibrated GCMC points for 1000 ps, were performed to this end, with a time step of 0.002 ps.

The selected thermostat points were handled by the velocity rescaling, *v*-rescale method,²⁹ and the bond and angles were constrained by the shake method.³⁰ Additionally, with nitrogen as the probe molecule, the 3D Particle Mesh Ewald method,^{31,32} with 0.12 Fourier spacing for the long-range electrostatics determination, was implemented.

GROMACS³³ and MuSiC²⁷ software were used for MD and GCMC simulations, respectively, and the VMD³⁴ package was used for the visualization and rendering of the snapshots.

3. RESULTS AND DISCUSSION

Single experimental adsorption isotherms of *n*-pentane and methylcyclohexane were determined at 298 K on three silica samples, as described in the Methodology, Aerosil200, Aerosil200(823), and

Aerosil200(1223), and the results are presented in Figures 1 and 2, respectively. One can notice that the thermal treatment of the silica does not significantly affect the overall VOC adsorption capacity. This allows us to use a recently proposed effective model surface for Aerosil200 samples,¹⁴ in which, we predicted, without further modification of its parameters, the VOC adsorption. In Figures 3 and 4, the single experimental and simulated adsorption isotherms determined at 298 K for *n*-pentane and methylcyclohexane, respectively, are compared.

It is evident that the *n*-pentane and methylcyclohexane model fluids predict the adsorption isotherms remarkably close at the low-pressure regime, below a relative pressure of ~ 0.6 , with a mean absolute error (MAE) $< 2\%$. The discrepancies found between experiments/simulations for both adsorbates, at higher relative pressures, can be attributed to the infinite size of the simulation cell, which is repeated (3 times unit cell) in the *xy* plane to mimic an infinite surface, and hence, neither edges nor intraparticle adsorption can be accounted for by this model.

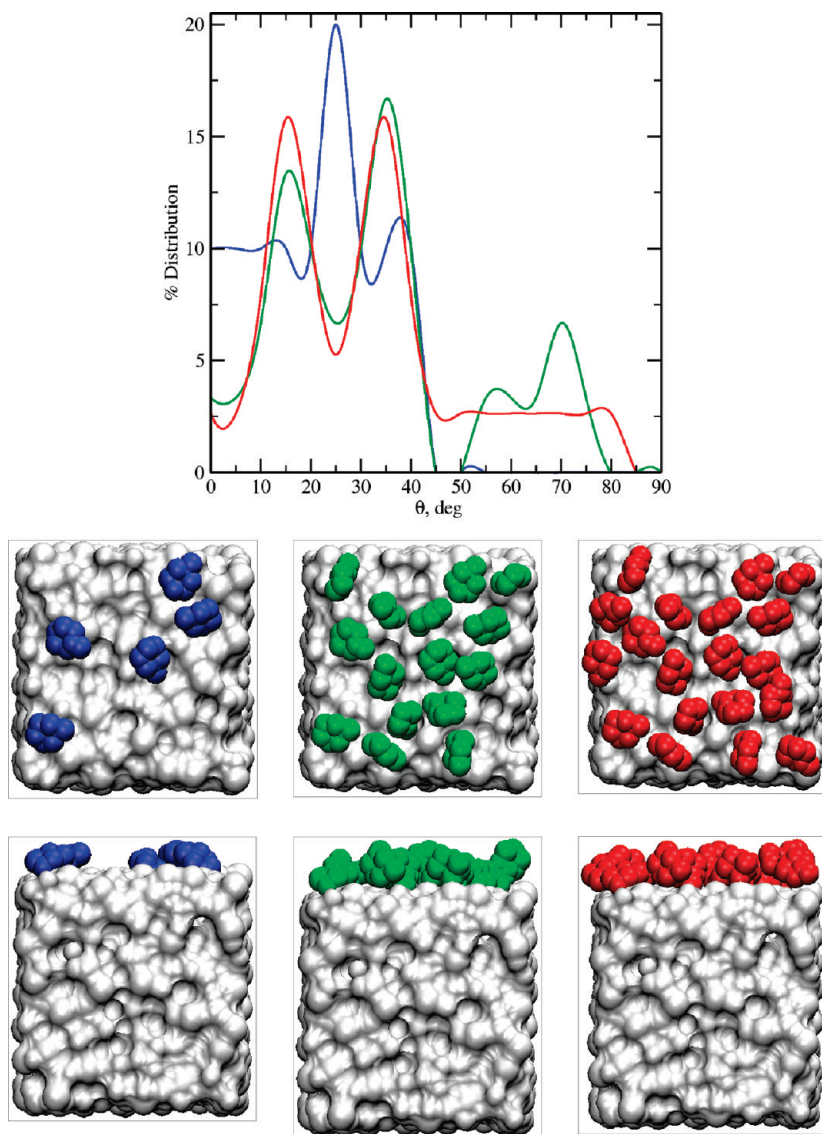


Figure 7. Percentage angle distribution for methylcyclohexane at 298 K on nonporous silica, following the description of Figure 6.

n-Pentane and methylcyclohexane adsorption simulations confirm our previous proposal¹⁴ that this type of effective model surface could be used for the description of VOC adsorption. It is worth stressing that the methylcyclohexane model used here was set as a rigid structure in the chair conformation with the methyl group at the equatorial position. A detailed study on the flexibility of this molecule was performed (results not shown here), under the hypothesis that a different model conformation (than that at the equilibrated fluid bulk) could be accomplished at the surface; however, relevant differences were not found.

The same molecular simulation framework, with the above explained characteristics, enables us to perform a landing angle analysis, as described in the Methodology. The selected adsorbates are nitrogen, *n*-pentane, and methylcyclohexane, i.e., the probe molecule used to tune the silica model and also the smallest molecule in the study and two different nonpolar adsorptives, *n*-pentane, larger than nitrogen but still linear, and methylcyclohexane, both a larger and wider molecule, at three different relative pressures (different surface coverage).

The results for the adsorbed nitrogen molecules at relative pressures of 1×10^{-5} , 4×10^{-3} , and 1×10^{-2} are presented in Figure 5. All pressure levels showed a wide and disperse angle distribution, although a few peaks can be distinguished as well as some general common features. All nitrogen distributions ranged mainly from ~ 0 to $\sim 60^\circ$, and they all have an average angle around 32° ($\pm 19.5^\circ$), with its standard deviation given in parentheses. These wide distributions are the result of the ability of nitrogen to explore every nook and cranny on the surface. The lowest relative pressure studied presented the contribution of angles $>60^\circ$, pinpointing the loci of hot spots in the surface, surface's valleys, in which, even at 80° with respect to the *xy* plane, the contact area of a nitrogen molecule is maximized (by solid–fluid interaction of perpendicular and lateral projections). However, at higher pressures, these contributions to the total angle distribution are diminished, because of the early occupancy of those hot spots and the increasing weight of smaller angles corresponding to flatter orientations. High contrast colored snapshots are also given for each relative pressure level studied, low (blue molecules),

medium (green molecules), and high (red molecules), against a white-colored surface, in zenithal and frontal viewer perspective.

n-Pentane is a more specific probe molecule for the distribution angle determination in comparison to nitrogen, in the sense that, as can be seen in Figure 6, with this adsorbate, the selected pressure level has a direct and differentiated influence on the characteristics of the distributions. At a relative pressure of 0.1, the lowest pressure studied for *n*-pentane, the average angle is $\sim 12^\circ$ ($\pm 10^\circ$), while the most relevant peak of the distribution can be found at $\sim 5^\circ$, representing ca. 37% of the molecules preferential orientation to the surface *xy* plane. Increasing the coverage, up to those corresponding to relative pressures of 0.2 and 0.3, has a proportional direct effect on the average angle of the distribution, with those being $\sim 15^\circ$ ($\pm 12^\circ$) and 30° ($\pm 24^\circ$), respectively. Landing angles $>60^\circ$ are just found at a relative pressure of 0.3, representing around 5% of the molecule population. Therefore, the preferential adsorption orientation for the *n*-pentane molecules is flat to the surface until a certain level of pressures (surface coverage) is imposed, allowing for steep angles to appear.

The methylcyclohexane-calculated angles are presented in Figure 7. In a similar fashion to the *n*-pentane distribution, a tendency from flatter to steeper orientations can be drawn as the pressure level is increased. The average angle varies from 19° ($\pm 13^\circ$) to 31° ($\pm 19^\circ$), when the relative pressure is increased from 0.1 to 0.3. For this probe molecule, the presence of angles $>60^\circ$ are found given a certain pressure level, in this case, relative pressure of 0.2, representing less than 7% of the molecules in the surface.

It is worth noticing that both VOCs, *n*-pentane and methylcyclohexane, presented a surface angle increase with the pressure behavior, implying that, for these two probe molecules, a certain contribution from the fluid–fluid interaction is needed before higher angles are achieved.

Finally, when the snapshots for the three different adsorbates are compared, one can see that, despite the fact of these molecules being in front of the same surface, each one defined very different hot spots. In other words, the preferential adsorption loci strongly depends upon the shape of the adsorptive and the partial surface coverage; therefore, they are not intrinsic to the surface. In the same way, when the angle distributions are compared, the nitrogen molecules will describe the studied surface as a surface having a higher roughness than that of the *n*-pentane or methylcyclohexane molecules, because nitrogen, being the smaller probe molecule of the study, will be able to explore a more extended area than the other two probe molecules and can sense places where *n*-pentane or methylcyclohexane cannot gain access.

4. CONCLUSION

Nowadays, the synergies between experimental techniques and molecular simulation tools can provide a vehicle to approach the adsorption systems in a closer way. With the presented methodology applied further in a statistically relevant study, with many more surface determinations, one can parametrize (in a mathematical sense) a function to relate the angle distribution with a corresponding surface roughness. Design tasks could benefit from the type of combined experimental/simulation strategy present here that will have ultimately a favorable impact in the cost of the units and the global health of the process and, nonetheless, in our understanding of a given specific adsorption system.

AUTHOR INFORMATION

Corresponding Author

*E-mail: cherdes@uevora.pt.

ACKNOWLEDGMENT

This work was financially supported by FEDER funds through the Programa Operacional Factores de Competitividade (COMPETE) and national funds through Fundação para a Ciéncia e a Tecnologia (FCT) under Projects FCOMP-01-0124-FEDER-007145 (PTDC/CTM/67314/2006) and PEst-OE/QUI/UI0619/2011.

REFERENCES

- (1) Khan, F. L.; Ghoshal, A. K. *J. Loss Prev. Process Ind.* **2000**, *13* (6), 527.
- (2) United States Environmental Protection Agency (U.S. EPA). *Technical Bulletin: Choosing an Adsorption System for VOC: Carbon, Zeolite, or Polymers?*; U.S. EPA: Washington, D.C., May 1999; EPA 456/F-99-004, www.epa.gov/ttn/catc/dir1/fadsorb.pdf.
- (3) Nguyen, C.; Sonwane, C. G.; Bhatia, S. K.; Do, D. D. *Langmuir* **1998**, *14*, 4950.
- (4) Trens, P.; Tanchoux, N.; Maldonado, D.; Galarneau, A.; Di Renzo, F.; Fajula, F. *New J. Chem.* **2004**, *28*, 874.
- (5) Das, D.; Gaur, V.; Verma, N. *Carbon* **2004**, *42*, 2949.
- (6) Qiao, S. Z.; Bhatia, S. K.; Nicholson, D. *Langmuir* **2004**, *20*, 389.
- (7) Ribeiro Carrott, M. M. L.; Russo, P. A.; Carvalhal, C.; Carrott, P. J. M.; Marques, J. P.; Lopes, J. M.; Gener, I.; Guisnet, M.; Ribeiro, F. R. *Microporous Mesoporous Mater.* **2005**, *81* (1–3), 259.
- (8) Ravikovitch, P. I.; Vishnyakov, A.; Neimark, A. V.; Ribeiro Carrott, M. M. L.; Russo, P. A.; Carrott, P. J. M. *Langmuir* **2006**, *22*, 513.
- (9) Herdes, C.; Valente, A.; Lin, Z.; Rocha, J.; Coutinho, J. A. P.; Medina, F.; Vega, L. F. *Langmuir* **2007**, *23* (13), 7299.
- (10) Herdes, C.; Sarkisov, L. *Langmuir* **2009**, *25* (9), 5352.
- (11) Coasne, B.; Alba-Simionescu, C.; Audonnet, F.; Dosseh, G.; Gubbins, K. E. *Langmuir* **2009**, *25*, 10648.
- (12) Findenegg, G. H.; Jahner, S.; Muter, D.; Prass, J.; Paris, O. *Phys. Chem. Chem. Phys.* **2010**, *12*, 7211.
- (13) Russo, P. A.; Ribeiro Carrott, M. M. L.; Carrott, P. J. M. *New J. Chem.* **2011**, *35* (2), 407.
- (14) Herdes, C.; Russo, P. A.; Ribeiro Carrott, M. M. L.; Carrott, P. J. M. *Adsorpt. Sci. Technol.* **2011**, *29* (4), 357.
- (15) Reid, R. C.; Prausnitz, J. M.; Poling, B. E. *The Properties of Gases and Liquids*; McGraw-Hill: New York, 1986.
- (16) Siboulet, B.; Coasne, B.; Dufreche, J. F.; Turq, P. *J. Phys. Chem. B* **2011**, *115*, 7881.
- (17) Feuston, B. P.; Garofalini, S. H. *J. Chem. Phys.* **1988**, *89*, 5818.
- (18) Rosenthal, A. R.; Garofalini, S. H. *J. Am. Ceram. Soc.* **1987**, *70*, 821.
- (19) Martin, M. G.; Siepmann, J. I. *J. Phys. Chem. B* **1998**, *102*, 2569.
- (20) Martin, M. G.; Siepmann, J. I. *J. Phys. Chem. B* **1999**, *103*, 4508.
- (21) Chen, B.; Siepmann, J. I. *J. Phys. Chem. B* **1999**, *103*, 5370.
- (22) Wick, C. D.; Martin, M. G.; Siepmann, J. I. *J. Phys. Chem. B* **2000**, *104*, 8008.
- (23) Chen, B.; Potoff, J. J.; Siepmann, J. I. *J. Phys. Chem. B* **2001**, *105*, 3093.
- (24) Lubna, N.; Kamath, G.; Potoff, J. J.; Rai, N.; Siepmann, J. I. *J. Phys. Chem. B* **2005**, *109*, 24100.
- (25) Rai, N.; Siepmann, J. I. *J. Phys. Chem. B* **2007**, *111*, 10790.
- (26) Allen, M. P.; Tildesley, D. J. *Computer Simulation of Liquids*; Clarendon Press: Oxford, U.K., 1987.
- (27) Gupta, A.; Chempath, S.; Sanborn, M. J.; Clark, L. A.; Snurr, R. Q. *Mol. Simul.* **2003**, *29*, 29.
- (28) Snurr, R. Q.; Bell, A. T.; Theodorou, D. N. *J. Phys. Chem.* **1993**, *97*, 13742.
- (29) Bussi, G.; Donadio, D.; Parrinello, M. *J. Chem. Phys.* **2007**, *126* No. 014101.

- (30) Ryckaert, J. P.; Ciccotti, G.; Berendsen, H. J. C. *J. Comput. Phys.* **1997**, *23*, 327.
- (31) Darden, T.; York, D.; Pedersen, L. *J. Chem. Phys.* **1993**, *98*, 10089.
- (32) Essmann, U.; Perera, L.; Berkowitz, M. L.; Darden, T.; Lee, H.; Pedersen, L. G. *J. Chem. Phys.* **1995**, *103*, 8577.
- (33) Lindahl, E.; Hess, B.; van der Spoel, D. *J. Mol. Model.* **2001**, *7*, 306.
- (34) Humphrey, W.; Dalke, A.; Schulten, K. *J. Mol. Graphics* **1996**, *14*, 33.